

# Automatic Tuberculosis Screening from Chest Radiographs using Neural Networks

Ajeena A

PG Scholar

Younus College of Engineering and Technology,  
Vadakkevila, Kollam-691010

Mrs. Jiji. N

Associate Professor ,CSE

Younus College of Engineering and Technology,  
Vadakkevila, Kollam-691010

**Abstract**-Tuberculosis is a major health threat in many regions of the world. Opportunistic infections in immune compromised HIV/AIDS patients and multi-drug-resistant bacterial strains have exacerbated the problem, while diagnosis in tuberculosis still remains a challenge. When left undiagnosed and thus untreated, mortality rates of patients with tuberculosis are high. Standard diagnostics still rely on methods developed in the last century. They are slow and often unreliable. In an effort to reduce the burden of the disease, this paper presents our automated approach for detecting tuberculosis in conventional posteroanterior chest radiographs. We first extract the lung region using a graph cut segmentation method. For this lung region, we compute a set of texture and shape features, which enable the X-rays to be classified as normal or abnormal using a binary classifier. The proposed computer-aided diagnostic system for TB screening, which is ready for field deployment, achieves a performance that approaches the performance of human experts. We achieve an area under the ROC curve (AUC) of 87% accuracy.

**Keywords**—Computer-aided detection and diagnosis, lung, pattern recognition and classification, segmentation, tuberculosis(TB), X-ray imaging.

## I. INTRODUCTION

Tuberculosis (TB) is a widespread disease caused by infection of a bacterium called Mycobacterium Tuberculosis. Mycobacterium tuberculosis which released when tubercular coughing can cause the tuberculosis disease to spread on another people. Mycobacterium tuberculosis enters and gathers in lungs then proliferates become much more.. TB bacteria can spread out through the blood vessel or the lymph gland, therefore tuberculosis disease needs to be coped and at the present become the attention in the world . It is most often found in the lungs .Most people who are exposed to TB never develop symptoms because the bacteria can live in an inactive form in the body. But if the immune system weakens, such as in people with HIV or elderly adults, TB bacteria can become active. In their active state, such as in people with HIV or elderly adults, TB bacteria can become active. In their active state, TB bacteria cause death of tissue in the organs they infect. Active TB disease can be fatal if left untreated.

TB is the second leading cause of death from an infectious disease worldwide, after HIV, with a mortality rate of over 1.2 million people in 2010[1]. It is found that one-third of the world's population are carriers of this

disease, originating about 10 million cases of active TB worldwide and approximately 2 million deaths annually. The main cause of the infection can be due the increasing susceptibility of human population affected by AIDS, poverty, other factors weakening the immune systems of populations in developing countries and the socially marginalised groups in developed countries. The disease can affect different parts of body such as lungs, kidneys, liver, bones, brains and central nervous system. Pulmonary TB (PTB) refers to TB disease inside the lungs and is the most common type of TB. Extra pulmonary TB (EPTB) refers to TB disease outside the lungs. TB disease is curable; early detection and treatment are the effective methods to reduce the mortality rate from TB and control the spread of the disease. Manual examination of TB bacilli under the microscope remains the most widely used test for clinical diagnosis of TB. However, shortage of medical facilities and human expertise are the main limitations associated with the early detection. In case of PTB, the diagnosis is based on sputum smear examination, while EPTB is diagnosed by using tissue histology. The task is tedious, time consuming and subject to human error.

In this paper, we present an automated approach for detecting TB manifestations in chest X-rays (CXRs), based on our earlier work in lung segmentation and lung disease classification[4]-[6] . An automated approach to X-ray reading allows mass screening of large populations that could not be managed manually. A posteroanterior[7] radiograph (X-ray) of a patient's chest is a mandatory part of every evaluation for TB . The chest radiograph includes all thoracic anatomy and provides a high yield, given the low cost and single source[8]. Therefore, a reliable screening system for TB detection using radiographs would be a critical step towards more powerful TB diagnostics.

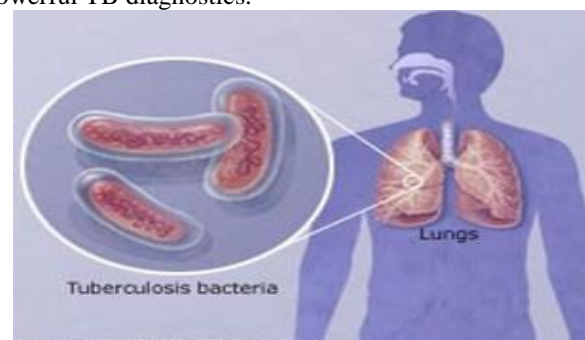


Fig.1 Tuberculosis

## II. RELATED WORKS

There are several TB tests available to diagnosis TB. There are also TB tests to find out whether someone has TB bacteria that are susceptible to TB drug treatment or are drug resistant. TB tests to find out if someone has drug resistant TB, are known as drug susceptibility test. The commonly used TB tests are TB skin test, interferon gamma release assays, culturing bacteria, sputum smear microscopy, polymerase chain reaction. These tests give good results but they are time consuming, sometimes subjects to human mistakes and the cost for these tests are high. So we introduce Computer Aided Diagnosis (CAD) as a second opinion for finalizing the results.

In radiology, computer-aided detection (CADe), also called computer-aided diagnosis (CADx), are procedures in medicine that assist doctors in the interpretation of medical images. Imaging techniques in X-ray, MRI, and Ultrasound diagnostics yield a great deal of information, which the radiologist has to analyze and evaluate comprehensively in a short time. CAD systems help scan digital images, e.g. from computed tomography, for typical appearances and to highlight conspicuous sections, such as possible diseases.

In recent years, due to the complexity of developing full-fledged CAD systems for X-ray analysis, research has concentrated on developing solutions for specific subproblems [14]-[21]. The segmentation of the lung field is a typical task that any CAD system needs to support for a proper evaluation of CXRs. Other segmentations that may be helpful include the segmentation of the ribs, heart, and clavicles [21]. For example, van Ginneken et al. compared various techniques for lung segmentation, including active shapes, rule-based methods, pixel classification, [21], [22] and various combinations thereof. Their conclusion was that pixel classification provided very good performance on their test data. Dawoud presented an iterative segmentation approach that combines intensity information with shape priors trained on the publicly available JSRT database [24].

Depending on the lung segmentation, different feature types and ways to aggregate them have been reported in the literature. For example, van Ginneken et al. subdivide the lung into overlapping regions of various sizes and extract features from each region. To detect abnormal signs of diffuse textural nature they use the moments of responses to a multiscale filter bank. In addition, they use the difference between corresponding regions in the left and right lung fields as features. A separate training set is constructed for each region [25] and classification is done by voting and a weighted integration.

Many of the CAD papers dealing with abnormalities in chest radiographs do so without focusing on any specific disease. Only a few CAD systems specializing in TB detection have been published, such as. [25]-[28] For example, Hogeweg et al. combined a texture-based abnormality detection system with a clavicle detection stage to suppress false positive responses [26]. In, [29] the same group uses a combination of pixel classifiers and active shape models for clavicle segmentation. Note that the clavicle region is a notoriously

difficult region for TB detection because the clavicles can obscure manifestations of TB in the apex of the lung. Freedman et al. showed in a recent study that an automatic suppression of ribs and clavicles in CXRs can significantly increase a radiologist's performance for nodule detection. [30] A cavity in the upper lung zones is a strong indicator that TB has developed into a highly infectious state. [27] Shen et al. therefore developed a hybrid knowledge-based Bayesian approach to detect cavities in these regions automatically. Xu et al. [28] approached the same problem with a model-based template matching technique, with image enhancement based on the Hessian matrix. Arzhaeva et al. use dissimilarity-based classification to cope with CXRs for which the abnormality is known but the precise location of the disease is unknown. They report classification rates comparable to rates achieved with region classification on CXRs with known disease locations. More information on existing TB screening systems can be found in our recent survey. [32]

## III. THE PROPOSED PROTOCOL

This section presents our implemented methods for lung segmentation, feature computation, and classification. Fig. 2 shows the architecture of our system with the different processing steps, which the following sections will discuss in more detail. First, preprocess the image for removing the noises. our system segments the lung of the input CXR using a graph cut optimization method in combination with a lung model. For the segmented lung field, our system then computes a set of features as input to a pre-trained classifier. Finally, using decision rules and thresholds, the classifier outputs its confidence in classifying the input CXR as a TB positive case.

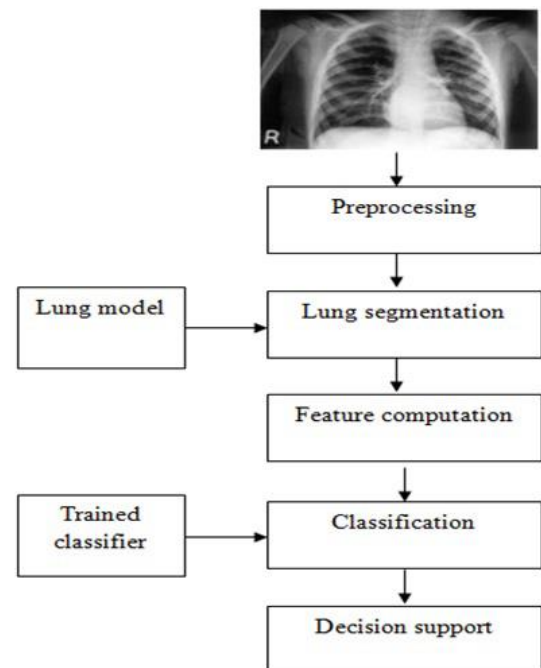


Fig2. System Overview

A. Preprocessing

Image preprocessing is the name for operations on images at the lowest level of abstraction whose aim is an improvement of the image data that suppress undesired distortions or enhances some image features important for further processing. It does not increase image information content. Its methods use the considerable redundancy in images. Neighboring pixels corresponding to one object in real images have the same or similar brightness value and if a distorted pixel can be picked out from the image, it can be restored as an average value of neighboring pixels. Here we perform some operations such as binarization, complement, dilation, erosion.

Image binarization converts an image of up to 256 gray levels to a black and white image. The simplest way to use image binarization is to choose a threshold value, and classify all pixels with values above this threshold as white, and all other pixels as black. The problem then is how to select the correct threshold. In many cases, finding one threshold compatible to the entire image is very difficult, and in many cases even impossible. Therefore, adaptive image binarization is needed where an optimal threshold is chosen for each image area. The complement of an image means the output image is the reversal of the input image. In the case of an 8-bit image, the pixels with a value of 0 take on a new value of 255, while the pixels with a value of 255 take on a new value of 0. All the pixel values in between take on similarly reversed new values. The new image appears as the opposite of the original. The most basic morphological operations are dilation and erosion. Dilation adds pixels to the boundaries of objects in an image, while erosion removes pixels on object boundaries. The number of pixels added or removed from the objects in an image depends on the size and shape of the structuring element used to process the image. In the morphological dilation and erosion operations, the state of any given pixel in the output image is determined by applying a rule to the corresponding pixel and its neighbors in the input image. The rule used to process the pixels defines the operation as a dilation or an erosion. This table lists the rules for both dilation and erosion.

B. Graph Cut Based Lung Segmentation

We model lung segmentation as an optimization problem that takes properties of lung boundaries, regions, and shapes into account. [4] In general, segmentation in medical images has to cope with poor contrast, acquisition noise due to hardware constraints, and anatomical shape variations. Lung segmentation is no exception in this regard. We therefore incorporate a lung model that represents the average lung shape of selected training masks. We select these masks according to their shape similarity as follows. We first linearly align all training masks to a given input CXR. Then, we compute the vertical and horizontal intensity projections of the histogram equalized images. To measure the similarity between projections of the input CXR and the training CXRs, we use the Bhattacharyya coefficient. We then use the average mask computed on a subset of the most similar

training masks as an approximate lung model for the input CXR. In particular, we use a subset containing the five most similar training masks to compute the lung model.

This empirical number produced the best results in our experiments. Increasing the subset size to more than five masks will decrease the lung model accuracy because the shapes of the additional masks will typically differ from the shape of the input X-ray. As training masks, we use the publicly available JSRT set for which ground truth lung masks are available. [22] The pixel intensities of the lung model are the probabilities of the pixels being part of the lung field. Fig. 5 shows a typical lung model we computed. Note that the ground-truth masks do not include the posterior inferior lung region behind the diaphragm. Our approach, and most segmentation approaches in the literature, exclude this region because manifestations of TB are less likely here.

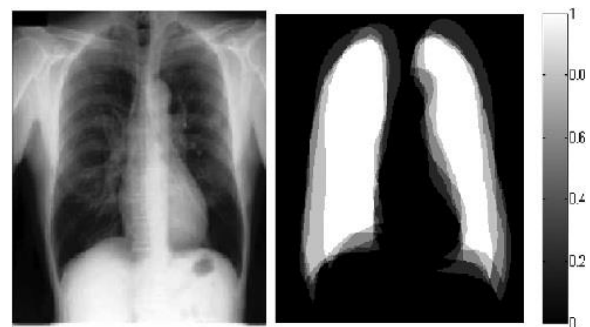


Fig 3. CXR and its calculated lung model

In a second step, we employ a graph cut approach and model the lung boundary detection with an objective function. To formulate the objective function, we define three requirements a lung region has to satisfy: 1) the lung region should be consistent with typical CXR intensities expected in a lung region, 2) neighboring pixels should have consistent labels, and 3) the lung region needs to be similar to the lung model we computed. Mathematically, we can describe the resulting optimization problem as follows:  $f = \{f_1, f_2, \dots, f_p, \dots, f_N\}$  a binary vector whose components  $f_p$  correspond to foreground (lung region) and background label assignments to pixel  $p \in P$ , where  $P$  is the set of pixels in the CXR, and  $N$  is the number of pixels. According to our method, the optimal configuration of  $f$  is given by the minimization of the following objective function.

$$E(f) = E_d(f) + E_s(f) + E_m(f)$$

Where  $E_d, E_s, E_m$  and represent the region, boundary, and lung model properties of the CXR, respectively.

C. Features

To describe normal and abnormal patterns in the segmented lung field, we use some features. The first set is a combination of shape, edge, and texture descriptors [6]. For each descriptor, we compute a histogram that shows the distribution of the different descriptor values across the lung field. Each histogram bin is a feature, and all features of all descriptors put together form a feature vector that we input to our classifier. Through empirical experiments, we

found that using 32 bins for each histogram gives us good practical results. In particular, we use the following shape and texture descriptors.

- Intensity histograms (IH).
- Gradient magnitude histograms (GM).
- Shape descriptor histograms (SD).
- Histogram of oriented gradients (HOG) is a descriptor for gradient orientations

weighted according to gradient magnitude. The image is divided into small connected regions, and for each region a histogram of gradient directions or edge orientations for the pixels within the region is computed. The combination of these histograms represents the descriptor. HOG has been successfully used in many detection systems.

#### D. Classification

Here the Artificial Neural Network is used for the classification. Artificial neural networks are relatively crude electronic networks of neurons based on the neural structure of the brain. They process records one at a time, and learn by comparing their classification of the record (i.e., largely arbitrary) with the known actual classification of the record. The errors from the initial classification of the first record is fed back into the network, and used to modify the networks algorithm for further iterations.

Neurons are organized into layers: input, hidden and output. The input layer is composed not of full neurons, but rather consists simply of the record's values that are inputs to the next layer of neurons. The next layer is the hidden layer. Several hidden layers can exist in one neural network. The final layer is the output layer, where there is one node for each class. A single sweep forward through the network results in the assignment of a value to each output node, and the record is assigned to the class node with the highest value. ANN gives the most accurate result for the classification such as the input CXR is normal or abnormal.

#### IV. RESULTS

Here we evaluate the performance of our work. We also compare the performance of our proposed TB detection system with the performance of systems reported in the literature, including the performance of human experts. In our study, we asked the radiologist to provide a reading for our CXR set. After the individual readings of radiologists we found that the false positives and the false negatives are evenly distributed, with a sensitivity of 74.1% and a specificity of 81.3%. This is because we have not optimized the true positive rate for our classifier. Finally, we compare the correct and incorrect classification results of the radiologist and the machine. In terms of classification performance, the radiologist are not significantly better than the machine. Note that the number of CXRs for which both the machine and the consensus are wrong is remarkably low. The combined human-machine performance with a significantly lower error rate of 4.3%, compared to the machine-only error rate of 21.7% and the human consensus error of 18.1%, suggests using our system for computer-aided diagnosis and verifying second opinion of radiologist readings. This can help improve human

performance because it is unlikely that both the radiologist and the machine classify the same CXR incorrectly.

#### V. CONCLUSION

We have developed an automated system that screens CXRs for manifestations of TB. The system is currently set up for practical use in Kenya, where it will be part of a mobile system for TB screening in remote areas. When given a CXR as input, our system first segments the lung region using an optimization method based on graph cut. This method combines intensity information with personalized lung atlas models derived from the training set. We compute a set of shape, edge, and texture features as input to a binary classifier, which then classifies the given input image into either normal or abnormal. The likelihood that the radiologist and the machine reach a wrong conclusion is very low. This shows that it should be possible to reach human performance in the future, or at least have a system that can assist radiologists and public health providers in the screening and decision process. These comparison results have encouraged us to test our system in the field under realistic conditions.

#### REFERENCE

- [1] World Health Org., Global tuberculosis report 2012.
- [2] World Health Org., Global tuberculosis control 2011 2011.
- [3] Stop TB Partnership, World Health Org., The Global Plan to Stop TB 2011–2015 2011.
- [4] S. Candemir, S. Jaeger, K. Palaniappan, S. Antani, and G. Thoma, "Graph-cut based automatic lung boundary detection in chest radiographs," in *Proc. IEEE Healthcare Technol. Conf.: Translat. Eng. Health Med.*, 2012, pp. 31–34.
- [5] S. Candemir, K. Palaniappan, and Y. Akgul, "Multi-class regularization parameter learning for graph cut image segmentation," in *Proc. Int. Symp. Biomed. Imag.*, 2013, pp. 1473–1476.
- [6] S. Jaeger, A. Karargyris, S. Antani, and G. Thoma, "Detecting tuberculosis in radiographs using combined lung masks," in *Proc. Int. Conf. IEEE Eng. Med. Biol. Soc.*, 2012, pp. 4978–4981.
- [7] C. Leung, "Reexamining the role of radiography in tuberculosis case finding," *Int. J. Tuberculosis Lung Disease*, vol. 15, no. 10, pp. 1279–1279, 2011.
- [8] L. R. Folio, *Chest Imaging: An Algorithmic Approach to Learning*. New York: Springer, 2012.
- [9] S. Jaeger, S. Antani, and G. Thoma, "Tuberculosis screening of chest radiographs," in *SPIE Newsroom*, 2011.
- [10] C. Daley, M. Gotway, and R. Jasmer, "Radiographic manifestations of tuberculosis," in *A Primer for Clinicians*. San Francisco, CA: Curry International Tuberculosis Center, 2009.
- [11] J. Burrill, C. Williams, G. Bain, G. Conder, A. Hine, and R. Misra, "Tuberculosis: A radiologic review," *Radiographics*, vol. 27, no. 5, pp. 1255–1273, 2007.
- [12] R. Gie, *Diagnostic Atlas of Intrathoracic Tuberculosis in Children*. International Union Against Tuberculosis and Lung Disease (IUATLD), 2003.
- [13] A. Leung, "Pulmonary tuberculosis: The essentials," *Radiology*, vol. 210, no. 2, pp. 307–322, 1999.
- [14] B. van Ginneken, L. Hogeweg, and M. Prokop, "Computer-aided diagnosis in chest radiography: Beyond nodules," *Eur. J. Radiol.*, vol. 72, no. 2, pp. 226–230, 2009.
- [15] G. Lodwick, "Computer-aided diagnosis in radiology: A research plan," *Invest. Radiol.*, vol. 1, no. 1, p. 72, 1966.
- [16] G. Lodwick, T. Keats, and J. Dorst, "The coding of Roentgen images for computer analysis as applied to lung cancer," *Radiology*, vol. 81, no. 2, p. 185, 1963.
- [17] S. Sakai, H. Soeda, N. Takahashi, T. Okafuji, T. Yoshitake, H. Yabuuchi, I. Yoshino, K. Yamamoto, H. Honda, and K. Doi,

- “Computer-aided nodule detection on digital chest radiography: Validation test on consecutive T1 cases of resectable lung cancer,” *J. Digit. Imag.*, vol. 19, no. 4, pp. 376–382, 2006.
- [18] J. Shiraishi, H. Abe, F. Li, R. Engelmann, H. MacMahon, and K. Doi, “Computer-aided diagnosis for the detection and classification of lung cancers on chest radiographs: ROC analysis of radiologists’ performance,” *Acad. Radiol.*, vol. 13, no. 8, pp. 995–1003, 2006.
- [19] S. Kakeda, J. Moriya, H. Sato, T. Aoki, H. Watanabe, H. Nakata, N. Oda, S. Katsuragawa, K. Yamamoto, and K. Doi, “Improved detection of lung nodules on chest radiographs using a commercial computer-aided diagnosis system,” *Am. J. Roentgenol.*, vol. 182, no. 2, pp. 505–510, 2004.
- [20] K. Doi, “Current status and future potential of computer-aided diagnosis in medical imaging,” *Br. J. Radiol.*, vol. 78, no. 1, pp. 3–19, 2005.
- [21] B. Van Ginneken, B. ter Haar Romeny, and M. Viergever, “Computer-aided diagnosis in chest radiography: A survey,” *IEEE Trans. Med. Imag.*, vol. 20, no. 12, pp. 1228–1241, Dec. 2001.
- [22] B. Van Ginneken, M. Stegmann, and M. Loog, “Segmentation of anatomical structures in chest radiographs using supervised methods: A comparative study on a public database,” *Med. Image Anal.*, vol. 10, no. 1, pp. 19–40, 2006.
- [23] B. van Ginneken and B. ter Haar Romeny, “Automatic segmentation of lung fields in chest radiographs,” *Med. Phys.*, vol. 27, no. 10, pp. 2445–2455, 2000.
- [24] A. Dawoud, “Fusing shape information in lung segmentation in chest radiographs,” *Image Anal. Recognit.*, pp. 70–78, 2010.
- [25] B. van Ginneken, S. Katsuragawa, B. ter Haar Romeny, K. Doi, and M. Viergever, “Automatic detection of abnormalities in chest radiographs using local texture analysis,” *IEEE Trans. Med. Imag.*, vol. 21, no. 2, pp. 139–149, Feb. 2002.
- [26] L. Hogeweg, C. Mol, P. de Jong, R. Dawson, H. Ayles, and B. van Ginneken, “Fusion of local and global detection systems to detect tuberculosis in chest radiographs,” in *Proc. MICCAI*, 2010, pp. 650–657.
- [27] R. Shen, I. Cheng, and A. Basu, “A hybrid knowledge-guided detection technique for screening of infectious pulmonary tuberculosis from chest radiographs,” *IEEE Trans. Biomed. Eng.*, vol. 57, no. 11, pp. 2646–2656, Nov. 2010.
- [28] T. Xu, I. Cheng, and M. Mandal, “Automated cavity detection of infectious pulmonary tuberculosis in chest radiographs,” in *Proc. Int. IEEE Eng. Med. Biol. Soc.*, 2011, pp. 5178–5181.
- [29] L. Hogeweg, C. I. Sánchez, P. A. de Jong, P. Maduskar, and B. van Ginneken, “Clavicle segmentation in chest radiographs,” *Med. Image Anal.*, vol. 16, no. 8, pp. 1490–1502, 2012.
- [30] M. Freedman, S. Lo, J. Seibel, and C. Bromley, “Lung nodules: Improved detection with software that suppresses the rib and clavicle on chest radiographs,” *Radiology*, vol. 260, no. 1, pp. 265–273, 2011.
- [31] Y. Arzhaeva, D. Tax, and B. Van Ginneken, “Dissimilarity-based classification in the absence of local ground truth: Application to the diagnostic interpretation of chest radiographs,” *Pattern Recognit.*, vol. 42, no. 9, pp. 1768–1776, 2009.
- [32] S. Jaeger, A. Karargyris, S. Candemir, J. Siegelman, L. Folio, S. Antani, and G. Thoma, “Automatic screening for tuberculosis in chest radiographs: A survey,” *Quant. Imag. Med. Surg.*, vol. 3, no. 2, pp. 89–99, 2013.
- [33] C. Pangilinan, A. Divekar, G. Coetzee, D. Clark, B. Fourie, F. Lure, and S. Kennedy, “Application of stepwise binary decision classification for reduction of false positives in tuberculosis detection from smeared slides,” presented at the Int. Conf. Imag. Signal Process. Healthcare Technol., Washington, DC, 2011.
- [34] C. Boehme, P. Nabeta, D. Hillemann, M. Nicol, S. Shenai, F. Krapp, J. Allen, R. Tahirli, R. Blakemore, and R. Rustomjee *et al.*, “Rapid molecular detection of tuberculosis and rifampin resistance,” *New Eng. J. Med.*, vol. 363, no. 11, pp. 1005–1015, 2010.
- [35] J. Shiraishi, S. Katsuragawa, J. Ikezoe, T. Matsumoto, T. Kobayashi, K. Komatsu, M. Matsui, H. Fujita, Y. Kodera, and K. Doi, “Development of a digital image database for chest radiographs with and without a lung nodule,” *Am. J. Roentgenol.*, vol. 174, no. 1, pp. 71–74, 2000.
- [36] Y. Boykov and G. Funka-Lea, “Graph cuts and efficient n-d image segmentation,” *Int. J. Comput. Vis.*, vol. 70, pp. 109–131, 2006.
- [37] Y. Boykov, O. Veksler, and R. Zabih, “Fast approximate energy minimization via graph cuts,” *IEEE Trans. Pattern Anal. Mach. Intell.*, vol. 23, no. 11, pp. 1222–1239, Nov. 2001.
- [38] S. Jaeger, C. Casas-Delucchi, M. Cardoso, and K. Palaniappan, “Dual channel colocalization for cell cycle analysis using 3D confocal microscopy,” in *Proc. Int. Conf. Pattern Recognit.*, 2010, pp. 2580–2583.
- [39] S. Jaeger, C. Casas-Delucchi, M. Cardoso, and K. Palaniappan, “Classification of cell cycle phases in 3D confocal microscopy using PCNA and chromocenter features,” in *Proc. Indian Conf. Comput. Vis., Graph., Image Process.*, 2010, pp. 412–418.
- [40] K. Palaniappan, F. Bunyak, P. Kumar, I. Ersoy, S. Jaeger, K. Ganguli, A. Haridas, J. Fraser, R. Rao, and G. Seetharaman, “Efficient feature extraction and likelihood fusion for vehicle tracking in low frame rate airborne video,” in *Proc. Int. Conf. Inf. Fusion*, 2010, pp. 1–8.
- [41] M. Linguraru, S. Wang, F. Shah, R. Gautam, J. Peterson, W. Linehan, and R. Summers, “Computer-aided renal cancer quantification and classification from contrast-enhanced CT via histograms of curvature-related features,” in *Proc. Int. Conf. IEEE Eng. Med. Biol. Soc.*, 2009, pp. 6679–6682.
- [42] R. Pelapur, S. Candemir, F. Bunyak, M. Poostchi, G. Seetharaman, and K. Palaniappan, “Persistent target tracking using likelihood fusion in wide-area and full motion video sequences,” in *Proc. Int. Conf. Inf. Fusion*, 2012, pp. 2420–2427.
- [43] N. Dalal and B. Triggs, “Histograms of oriented gradients for human detection,” in *Proc. Int. Conf. Comp. Vis. Patt. Recognit.*, 2005, vol. 1, pp. 886–893.
- [44] L. Chen, R. Feris, Y. Zhai, L. Brown, and A. Hampapur, “An integrated system for moving object classification in surveillance videos,” in *Proc. Int. Conf. Adv. Video Signal Based Surveill.*, 2008, pp. 52–59.
- [45] F. Han, Y. Shan, R. Cekander, H. Sawhney, and R. Kumar, “A two-stage approach to people and vehicle detection with HOG-based SVM,” in *Performance Metrics Intell. Syst. Workshop*, Gaithersburg, MD, 2006, pp. 133–140.
- [46] X. Wang, T. X. Han, and S. Yan, “An HOG-LBP human detector with partial occlusion handling,” in *Proc. Int. Conf. Comput. Vis.*, 2009, pp. 32–39.
- [47] T. Ojala, M. Pietikäinen, and T. Mäenpää, “Multiresolution gray-scale and rotation invariant texture classification with local binary patterns,” *IEEE Trans. Pattern Anal. Mach. Intell.*, vol. 24, no. 7, pp. 971–987, Jul. 2002.
- [48] T. Ojala, M. Pietikäinen, and D. Harwood, “A comparative study of texture measures with classification based on feature distributions,” *Pattern Recognit.*, vol. 29, pp. 51–59, 1996. JAEGER